Beitr. Phys. Atmosph., February 1988, p. 39–49
0005–8173/88/01 0039–11 $ 3.00/0

On the surface energy budget of coastal zones with tidal flats

M. Claussen
Forschungszentrum Geesthacht, Postfach 1160, D-2054 Geesthacht, Fed. Rep. Germany

(Manuscript received July, 1987; in revised form December, 1987)

Abstract

The surface energy budgets of marshy land and tidal flats have been studied by using a numerical model. The model is driven by meteorological data which were recorded off the German west coast at the end of June 1985.

The latent heat flux above marshy land is found to be much stronger than above tidal flats during the day. This difference is attributed to a larger hydrodynamic roughness of land surfaces. The soil heat flux of land surfaces exhibits a diurnal variation, whereas the soil heat flux of sandbars is controlled by the tides. During low tide the sensible heat flux is larger above sandbars than above marshy land. When inundated, sandbars give less sensible heat to the atmosphere than marshy land.

At night, only slight temperature contrasts between surfaces of open sea, tidal flats, and marshy land are observed during low tide. At high tide during a cloudless night, the temperature of coastal waters is a little bit larger than of open waters and marshy coast. By day, there is a smooth temperature gradient between cold open waters, warmer inundated tidal flats, and still warmer marshy coast. The exposed tidal flats may become a heat island between open waters and coast.

Local heating of tidal water turns out to be small during inundation and it is diminished or sometimes balanced out by advection.

Zusammenfassung

Zur Oberflächenenergiebilanz von tidebeeinflußten Küstengebieten

Die Oberflächenenergiebilanzen von Marschland und Wattgebiet wurden mit Hilfe eines numerischen Modells untersucht. In das Modell wurden meteorologischen Daten eingegeben, die vor der deutschen Nordseeküste Ende Juni 1985 gewonnen worden waren.

Die Rechnungen zeigen, daß tagsüber der latente Wärmestrom der Marschgebiete den der Wattgebiete bei weitem übertrifft. Dies wird der höheren hydrodynamischen Rauhigkeit der Landflächen zugerechnet. Der Bodenwärmestrom an Landoberflächen zeigt einen klaren Tagesgang, wohingegen in Wattgebieten der Tidezyklus die Phase des Bodenwärmestroms bestimmt. Der Fluß fühlbarer Wärme ist über trockengefallenen Sänden größer als über dem Marschland. Während der Flut kehrt sich dieses Verhältnis um.

Nachts, bei Ebbe, existiert nur ein geringer Unterschied in der Oberflächentemperatur der offenen Nordsee, des Watts und des Marschlandes. Während der nächtlichen Flutphase ist das Wasser über dem Watt ein wenig wärmer als die offene See und die Landoberfläche. Tagsüber zeichnet sich eine stetige Temperaturzunahme von der offenen See zum überfluteten Watt und schließlich zum Festland ab. Doch die trockengefallenen Sände können eine Wärmeinsel zwischen kalter offener See und dem Festland bilden.

Berechnungen des lokalen Wärmehaushaltes des Wasserkörpers über dem Wattgebiet zeigen, daß die lokale Erwärmung des Wasser durch Advektion vermindert oder in einigen Fällen sogar aufgehoben wird.

1 Introduction

The outstanding pecularity of the regional climate of coastal zones is the land/sea-breeze. The land/sea-breeze is primarily driven by horizontal gradients of temperature and energy fluxes over sea and land surfaces, respectively. Along the coast of the North Sea, zones with extended tidal flats are found which reach up to fifteen or twenty kilometers out into the sea. Here, the situation is more complex. Tidal inundation (or recession) may produce a significant horizontal displacement of zones of maximum temperature contrast.

By use of a 2-dimensional mesoscale model, Kessler et al. (1985) have found that a sea breeze adjust to tidal inundation. During low tide, the presence of a moist sandbar adjacent to the relatively dry land adds a boundary in addition to that between water and

sandbar, across which horizontal gradients of surface temperature develop and which can act to diffuse the sea-breeze. After complete inundation of sandbars, a significant surface temperature discontinuity is reported to exist only at the boundary between the inundated sandbar and the relatively hot land surface. Thus, inundation can both translate and intensify a sea breeze front.

The subject of this study is a reassessment of Kessler's et al. (1985) treatment of the surface energy budget of coastal zones with tidal flats. Kessler's et al. (1985) study is a purely theoretical one. Here, a combination of numerical simulation and experimental data is sought. Surface energy fluxes, surface temperature and moisture are computed by means of a simple model. The model is driven by meteorological data from two meteorological masts, which have been set up on the marshy island of 'Pellworm' and on a sandbar roughly 500 meters to the west of 'Pellworm'. The island is located approximately 15 kilometers off the coast of Nothern Germany (See Figure 1). The data were recorded from June 18th till July 2nd, 1985.

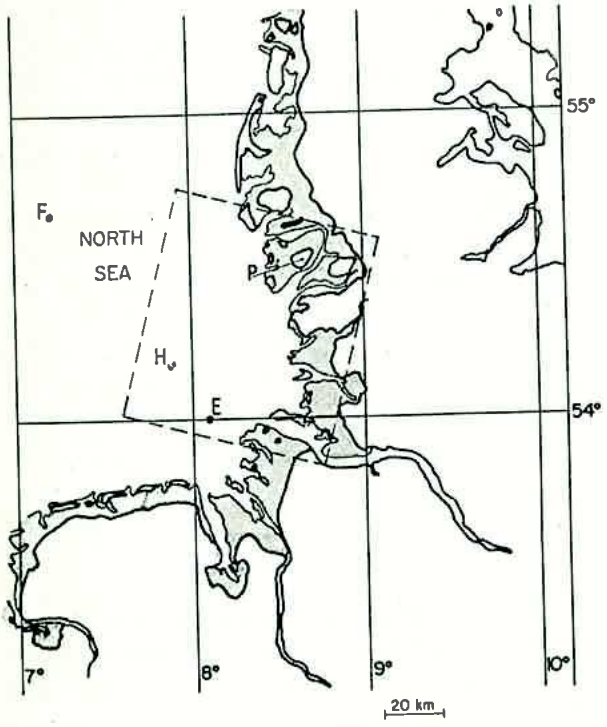

Figure 1 The North Sea coast of Germany. The sandbar areas are shaded. 'F' marks the location of the off-shore research station ‚Forschungplattform Nordsee', ‚E', of the light vessel ‚Elbe 1', ‚H', of the island of Helgoland, and ‚P', of the island of Pellworm. The dashed line shows the approximate location of the satellite picture figure 9

2 Model and Data

The surface temperature and surface humidity is evaluated by the requirement that no energy and no mass is stored at the interface between atmosphere and soil. The equation for the so-called surface energy balance reads, using symbolic notation:

$$Q_{rad} + Q_{lat} + Q_{sens} = Q_{soil} \tag{1}$$

and the surface water balance:

$$E_g - P = W_s. \tag{2}$$

The fluxes are considered positive when directed upward, and *vice versa.*

Q_{rad} is the sum of the following energy flux densities (dimension: W/m^2): (shortwave) global radiation R_s, reflected global radiation αR_s, (long-wave) atmospheric radiation R_l strikting the earth's surface, and radiation being emitted from that surface at a temperature T_G:

$$Q_{rad} = -R_s(1-\alpha) - \epsilon R_l + \epsilon\sigma T_G^4. \tag{3}$$

α is the albedo and ϵ is the mean emissivity of the earth's surface. σ is the Stefan-Boltzmann constant. In order to calculate R_s, the unattenuated solar radiation is computed and the attenuation due to turbidity and cloudiness is taken into account by Kasten and Czeplaks's (1980) parameterization. Their parameterization is valid for urban conditions. Therefore, Kasten and Czeplak's (1980) turbidity parameter has been adjusted to rural conditions by using data of solar radiation which were recorded at the island of Pellworm. A parameterization for R_l has been found in Deardorff (1978).

Q_{lat} and Q_{sens} stand for the energy flux densities due to turbulent transports of latent and sensible heat – in parametric notation:

$$Q_{lat} = -\rho L C_s u(z_a)\Delta q(z_a) \tag{4}$$

$$Q_{sens} = -\rho c_p C_s u(z_a)\Delta\Theta(z_a). \tag{5}$$

ρ is the air density, L is the latent heat of condensation, c_p is the specific heat of air at constant pressure, $u(z_a)$ is the mean wind speed at a height $z = z_a$ above ground, and $\Delta q(z_a)$ and $\Delta\Theta(z_a)$ are the differences of specific humidity q and potential temperature Θ, respectively, between heights $z = z_a$ and $z = z_0$. z_0 is the roughness length. The temperature and humidity difference between ground $z = 0$ and $z = z_0$ is calculated from Zilitinkevitch (1970).

C_s is the transfer coefficient of a scalar quantity. C_s is calculated by using Louis' (1979) parametric model. For some applications, the friction velocity u_* is computed. u_* is definded by

$$\tau(z = 0) = \rho u_*^2$$

where $\tau(z=0)$ is the bottom shear strees. The parametric estimation of u_* by

$$u_*^2 = C_D\, u^2(z_a)$$

is again taken from Louis (1979).

The last term in Eq. (1) is the soil heat flux:

$$Q_{soil} = -\lambda \left(\frac{\partial T}{\partial z}\right)_{z=0}, \qquad (6)$$

where λ ist the heat conductivity and T is the actual soil temperature.

In Eq. (2): E_g ist the evaporation rate (= Q_{lat}/L), P is the precipitation rate, and W_s is the flux of water and water vapor within the soil.

The influence of snow and ice on the surface temperature and surface humidity is not considered. Furthermore, the impact of geothermal and artifical heat sources on the surface energy fluxes will be neglected. Eq. (4) does not hold for vegetation.

Kessler et al. (1985) use McCumber and Pielke's (1981) simplified version of Philip's (1959) model of soil water and soil temperature transport. McCumber and Pielke's (1981) model takes into account the nonlinear interaction of soil temperature and soil moisture transport. In this study, a simpler approach has been chosen. The temperature transport within the soil is calculated from

$$\frac{\partial T}{\partial t} = \kappa \nabla^2 T. \qquad (7)$$

κ is the temperature conductivity with $\kappa = \lambda(\rho c)$, ρc being the soil heat capacity. Eg. (7) is solved by using an Euler scheme. The soil temperature T is defined at depths z = 0,-0.007,-0.018,-0.033,-0.053,-0.081,-0.120, -0.175,-0.252,-0.358,-0.506,-0.712,-1.000 m (z is positive upward; z = 0m corresponds to the air-soil interface). As boundary conditions for the calculation of soil temperature at a time step n, $T(z=0m)$ is taken as T_G^{n-1} of the previous time step and $T(z=-1m)$ is specified as a constant. (An implicit calculation with T_G^n as upper boundary condition turns out to not yield any differences provided that the time step is not larger than a few minutes.) Since no soil temperature had been recorded, $T(z=-1m) = 283.16K$ is arbitrarily assumed. This assumption is not a crucial one for short range forecasts. Sensitivity tests (not shown here) indicate that a variation of deep soil reference temperature by 10K yields a variation of approximately 3K at $z = -0.26m$ and almost none at the surface.

Eq. (7) is used only to compute Q_{soil} in Eq. (6). If the tidal flat becomes flooded, then the temperature of the water surface is not calculated from Eq. (1), but taken from measurements. Because the advection of water temperature as well as the turbulent mixing within the water is not known, the energy exchange at the air-water interface is estimated as a residual from $Q_{rad} + Q_{lat} + Q_{sens}$. During flood, Eq. (7) is used to estimate the temperature transport into the inundated tidal flat with the measured water temperature taken as boundary conditions at z = 0m. A possible change of soil temperature due to percolation of water into the sand is not taken into account.

The soil moisture transport is not computed. Instead, the surface humidity is diagnosed from

$$q_G = f q_s(T_G) + (1-f) q(z = z_a) \qquad (8)$$

where q_s, is the specific humidity at saturation and f is the so called surface wetness factor. f is computed from

$$\frac{\partial f}{\partial t} = -\frac{E_g - P}{w_k \rho_w}, \quad 0 \leqslant f \leqslant 1. \qquad (9)$$

ρ_w is the density of water, w_k is the critical depth of extracted liquid water that a thick upper layer of soil is capable of holding before the surface is saturated. Equations (8) and (9), and values of w_k are taken from Deardorff (1978).

Equations (7) and (9) are good estimates of soil temperature transport and surface humidity of sandbars, since sandbars are always saturated with water and, therefore, the heat conductivity λ is almost a constant with respect to depth (see Andrews, 1980).

Figure 2 (taken from Claussen, 1985) demonstrates that results of the simple model and of McCumber and Pielke's (1981) much more elaborate model compare favourably even when soil moisture varies drastically. The only difference between models is seen in Q_{rad}, the energy flux density of net radiation, and in Q_{sens}, the sensible heat flux, which presumably is caused by different specification of surface albedo. However, a word of caution has to be said. Claussen (1985, 1986) mentions that McCumber and Pielke's (1981) model may not properly describe soil hydraulics. Their model does not seem to simulate the so called 'evaporation barrier', a sudden reduction of evaporation which results in a abrupt increase in maximum surface temperature (compare with Sievers et al., 1983). Hence, a comparison of the simple model with McCumber and Pielke's (1981) model may be not a vigorous test, it merely ascertains similar performance.

Some confidence in the simple model may be gainted by studying Figure 3. Figure 3 shows a 12.5-day time series of specific humidity, which has been recorded within the upper portion of a grass canopy, and of specific humidity at the surface of a bare soil, which

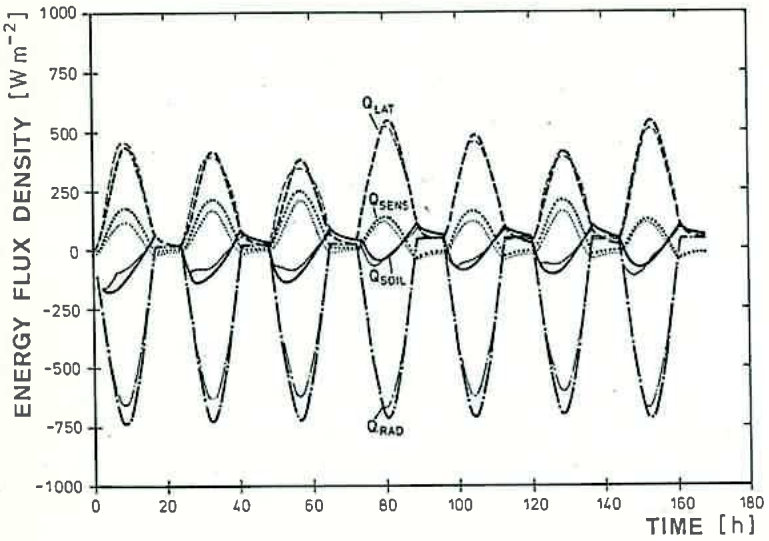

Figure 2

Energy flux density at a sand surface as function of time beginning at sun rise of the first day (3h:29min LST). Q_{lat} ist the energy flux of latend heat, Q_{sens} of sensible heat, Q_{soil} of soil heat, Q_{rad} of net-radiation.

The sand is saturated at the beginning of the first, the fouth, and the seventh day. Thick curves are results from the simple model, thin curves, from McCumber and Pielke's (1981) model.

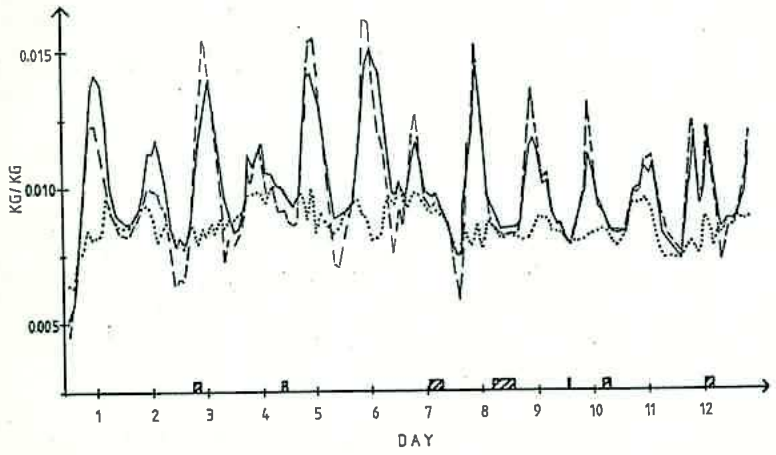

Figure 3

Specific humidity at the surface of clay pasture at the island of Pellworm during a period of 12.5 days beginning at June 19th, 1985. The abscissa indicates 12:00 LST of each day. Full line: model results, dashed line: observed data, dotted line: observed humidity approximartely three meters above ground.

The hatched areas indicate when rain was observed.

has been computed by the simple model. The model was driven by meteorological data of air temperature, humidity, wind speed, cloud cover, and precipitation which were measured roughly three meters above the grass canopy. Unfortunately, the temperature recording was slightly distored by an electronic failure. Hence, a quantitative comparison between model and experimental data is useless. On the other hand, the qualitative agreement between predicted and recorded humidity particularly when concerning the phase of both times series is satisfactory. Obviously, the simple model provides a fair prediction in cases of variable weather conditions.

In the following, recorded data of two days at the end of June 1985, indicated as days 5 and 6, are taken for a detailed discussion. During these days, the sky was cloudless; hence, pronounced temperature contrasts between water and land surfaces are to be expected.

3 Hydrodynamic and thermal properties

3a Hydrodynamic roughness

An obvious difference between marshy land and tidal flats is the difference in their hydrodynamic roughness. The hydrodynamic roughness can be expressed in terms of a roughness length z_0 (See Lumley and Panofsky, 1964, for instance). Over sea the roughness length depends on wind speed, which generates a more or less wavy, i.e. a more or less rough surface. A parametric formula is given by Clarke (1970):

$$z_0 = \begin{cases} 0.032\, u_*^2/g & u_* \geqslant 6.78\, 10^{-2}\,\mathrm{m/s} \\ 1.5\, 10^{-5} & u_* < 6.78\, 10^{-2}\,\mathrm{m/s} \end{cases} \qquad (10)$$

where g is the gravity acceleration and u_* the friction velocity.

The roughness length of a sandbar is chosen as z_0 = 0.0004m. This value is approcimately ten times as

large as the value found by Vugts and Cannemeijer (1981) from measurements over a smooth, flat sand surface. The factor of ten should take into account that a sandbar generally is not a flat surface, but exhibits small ripples which are created by wave motion.

The roughness length of marshy land is taken as $z_0 = 0.04$m. This value was computed from wind data, which were recorded at the mast at Pellworm. $z_0 = 0.04$m is the roughness length of a high-grown meadow or pasture-land.

3b Friction velocity

An immediate consequence of the difference in hydrodynamic roughness is the difference in friction velocity of marshy land, marine sand and open waters. Although the measured mean wind speed is stronger over tidal flats than over marshy land (see Figure 4), the friction velocity of open waters and of sandbars is smaller than over marshy land (see Figure 5). An increase in friction velocity implies an increase in turbulence and, obviously, in vertical turbulent transport of momentum. It is expected, that vertical turbulent transports of temperature and humidity are stronger over a rough surface than over a smooth surface provided that the gradients of these quantities do not differ drastically above rough and smooth surfaces.

3c Material constants

Albedo α, emissivity ϵ, temperature conductivity κ, and heat capacity ρc are taken from measurements of marine sands by Andrew (1980) and from Deardsdorff (1978) for clay pature and muddy water (See Table 1). Andrews (1980) data are in approximate agreement with those from Vugts and Zimmerman (1985). The albedo of water is parameterized by

$$\alpha = 0.25 - 0.23 \cos\theta \qquad (11)$$

where θ is the zenith angle of the sun. This parameterization is found from a figure in Andrews (1976). Of source, there is no unique type of marine sand.

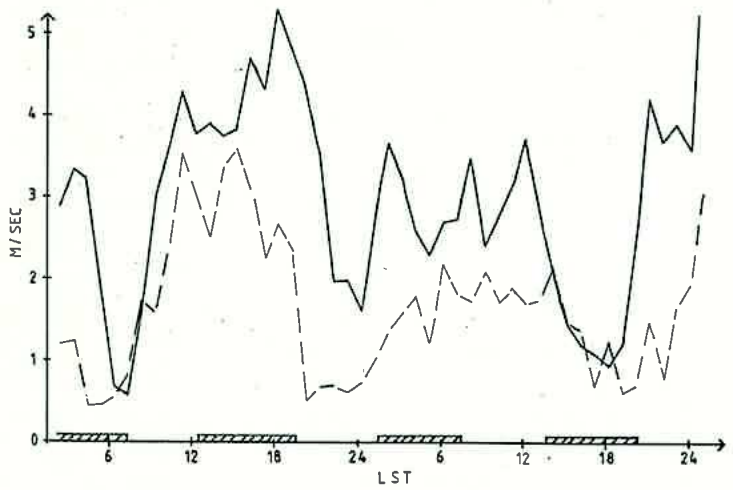

Figure 4
Wind speed measured approximately three above marshy land (dashed line) and tidal flats (full line) as function of local time during days 5 and 6 (Notation of day number as in Fig. 3). The hatched stripes indicate when the tidal flat is flooded.

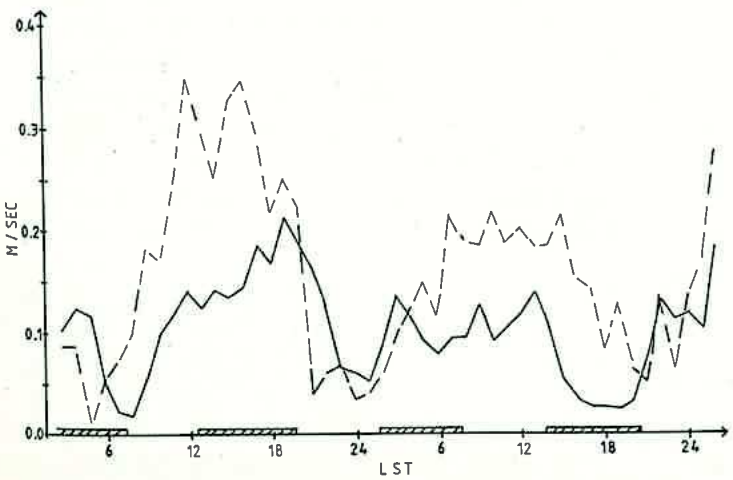

Figure 5
Same as Fig. 4, except for calculated friction velocity u_*.

Table 1 Physical parameters of soil and water
κ: temperature conductivity, ρc: heat capacity, ϵ: emissivity, α: albedo.
*: see text. Eq. (7).

	muddy water	wet marine sand	clay pasture
$\kappa[m^2/s\ 10^{-6}]$	0.15	0.51	1.2
$\rho c[J/(m^3K)\ 10^6]$	4.187	3.55	2.345
ϵ	0.94	0.91	0.95
α	*	0.12	0.15

However, use of one type or another does not strongly affect calculation of surface energy fluxes. The most significant difference between tidal flats and coast is the hydrodynamic roughness – as already mentioned – and the surface humidity. Even with strong evaporation, the relative humidity at the surface of a dry sandbar never falls below 99.8% during a low tide (Claussen, 1985).

For this study, the land surface is supposed to consist of marshy soil, i.e. loamy soil, clay pasture. Most of the land adjacent to tidal flats is marshy land, including the island where meteorological data were recorded.

4 Surface energy balance

4a Energy fluxes

The surface energy budget is depicted in Figure 6. The surface energy fluxes of marshy land and exposed tidal flats are calculated from Eq. (1). For the inundated tidal flat, however, the energy flux Q_{rad} due to net radiation, the latent heat flux Q_{lat}, and the sensible heat flux Q_{sens} are evaluated for the air-water interface at a constant water temperature T_G^w, which is taken from measurements. The heat flux from the air into the water, or *vice versa,* is not computed from Eq. (6), but estimated as a residual from the heat balance equation, because the temperature transport within the water is presumably dominated by (unknown) advection and turbulent mixing – not by molecular temperature diffusion. In Figure 6 this residual is not shown. Instead, in Figure 6, Q_{soil} is the heat flux at the water-soil interface, when the sandbar is inundated, and at the air-soil interface, when the sandbar is exposed. A discussion of the residual energy flux at the air-water interface will follow in Section 4c.

From Figure 6 it is seen that the energy flux Q_{rad} due to net radiations is similar over marshy land and over sandbars. When the sandbar becomes flooded, then – Q_{rad} gets stronger, presumably, because the albedo is reduced and because the cold water emits less infrared radiation.

The sensible heat flux Q_{sens} apparently contributes least to the surface energy budget. Q_{sens} is a little bit larger over a sandbar than over marshy land.

In the daytime, the latent heat flux Q_{lat} reveals the most drastic differences. Over marshy land Q_{lat} becomes roughly twice as large as over a dry sandbar and almost ten times as large as over an inundated sandbar. This is basically caused by the difference in friction velocity. That (relatively) cold water above the inundated sandbar evaporates less than a warm, humid land surface adds to this effect. Over tidal flats, the Brown ratio, i.e. the ratio of sensible to latent heat flux, amounts to 1/4 and, over marshy land, to 1/10. The latter value is in good agreement with measurements by Mast et al. (1984).

The soil heat flux Q_{soil} at the surface of a sandbar changes sign when the sandbar becomes flooded in the daytime. The heat being stored in the marine sand is diffused into the water above the sandbar. Whether this heat exchange can significantly en-

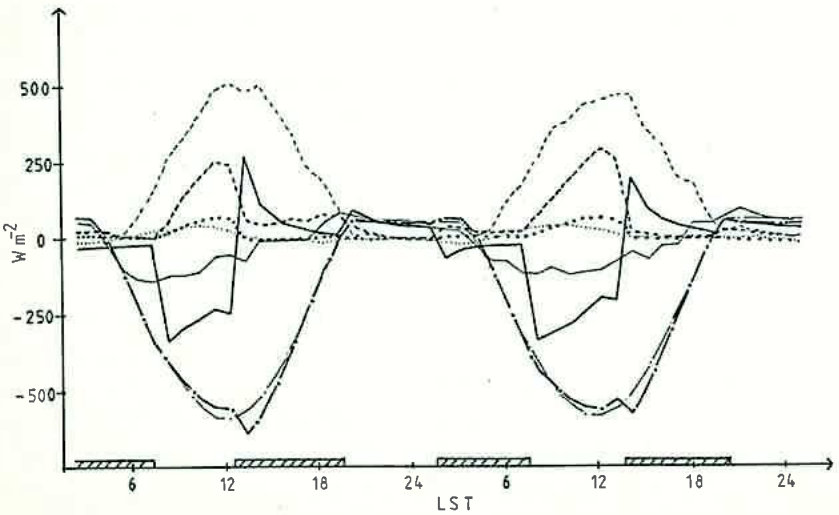

Figure 6
Same as Fig. 4, except for calculate budget of surface fluxes of tidal flats (thick lines) and of marshy land (thin lines). – – – energy flux of latent heat, ... of sensible heat, —— of soil heat, –.– of netradiation.

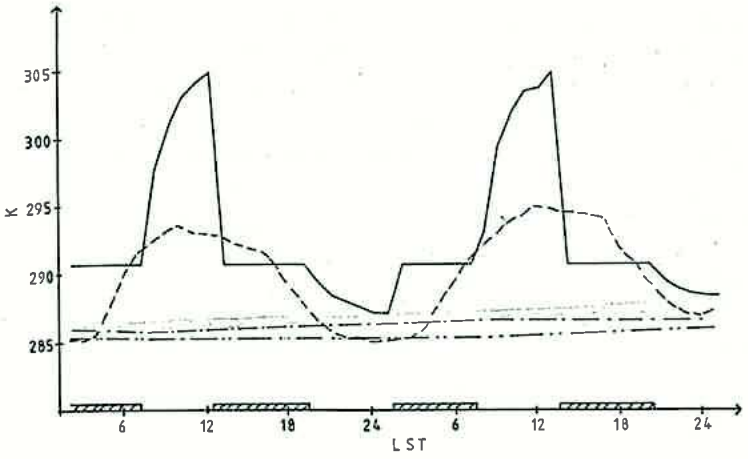

Figure 7

Same as Fig. 4, except for calculated surface temperature of tidal flats (full line) and of marshy land (dashed line) as well as temperature the at light vessel ‚Elbe 1' (dot-dashed line) and at the off-shore research station ‚Forschungsplattform Nordsee' (dot-dot-dashed line).

The latter data are daily 08.00 LST observations (connected by a straight line) taken from ‚Seewetterkarte' edited by ‚Deutscher Wetterdienst, Seewetteramt Hamburg'.

hance the water temperature will be studied in Section 4c. During the night and low tide the soil heat flux is directed upward. When the sandbar becomes inundated by night, then the relatively warm water heats the tidal flat. While the sign of Q_{soil} of tidal flats strongly depends on tidal inundation, the soil heat flux of marshy land varies more smoothly, being negative in the daytime and positive in the night.

4b Surface temperature

Figure 7 shows calculated surface temperatures of a tidal flat and marshy land as well as observed temperatures of open waters. The latter are taken from the light vessel 'Elbe 1' in the German Bight and the off-shore research station 'Forschungsplattform Nordsee' north-west of the island of Helgoland. In Figure 7 four distinct temperature regimes can be seen.

In the daytime and high tide, there is a smooth temperature gradient from cold open waters to warmer waters above sandbars and, further, to warmest land surfaces. At low tide, the tidal flat becomes warmest. Then the tidal flat is a heat island between cold open waters and warm land surfaces. During the night, the opposite is observed. At low tide only a slight temperature contrast is found. At high tide, however, the inundated sandbars can be viewed as a weak heat island.

The possibility of a daytime heat island induced by sandbars is predicted for variable weather conditions when land surfaces are moist. This is a new detail to be added to Kessler's et al. (1985) investigation. If the land surface consists of dry loam or of dry sand (dunes), then the dry tidal flats not necessarily induce a heat island, because the Bowen ratio over land surfaces could become larger than over tidal flats resulting in an increase of surface temperature. This effect is seen in Kessler's et al. (1985) study.

Finally, Kessler et al. (1985) neglect that the temperature of open water is not necessarily the same as that of water above tidal flats. They assume the same temperature for all water surfaces. Therefore, they report a steep temperature gradient between inundated tidal flats and land surfaces. As seen in Fig. 7, the water above inundated tidal flats can be much warmer than open waters. This can act to diffuse the horizontal temperature gradient, particularly during spring and early summer. The next section will provide a closer look into the latter detail.

4c Warming of tidal water

At the position of the data mast, the surface water temperature above the inundated tidal flat is held constant in the numerical model. Hence, it is assumed that advection of temperature as well as vertical mixing during advection balance out local heating by radiation or heat exchange with marine sands.

18 cases of daytime and night-time high tide periods have been used to test the assumption of constant water temperature. The temperature was measured approximately 0.03m below the water surface. Suggesting a linear trend $T = \alpha + \beta t$, where T is the temperature and t the time, the hypothesis $\beta = 0$ has been tested against $\beta \neq 0$ (the method is taken from Kreyszig, 1977). In 9 cases (from 18), the hypothesis $\beta = 0$ has to be rejected at the 5% significance level, and in 2 cases, at the 1% significance level. Hence, in~61% of all cases being investigated, the temperature trend is significantly different from zero. However, the trend is negilibly small in comparison with changes in surface temperature of dry sandbars and marshy land. An average variation of 0.4K and a maximum variation of 0.7K is found when a trend in water temperature is ignored- in the cases where statistics indicate a significant trend. In the other, ~39% of all cases,

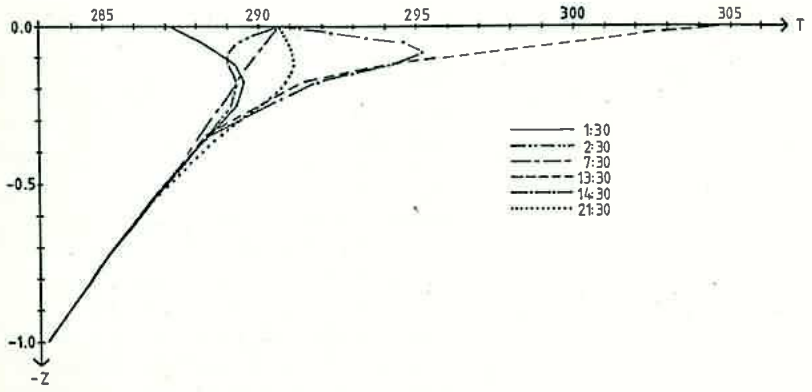

Figure 8
Predicted soil temperature of tidal flats as function of depth at day 6 (Notation of day number as in Fig. 3). Curve parameters indicate LST.

the temperature trend is so small (average variation ~0.1K) that the hypothesis $\beta = 0$ is acceptable. Thus, for many applications in mesoscale meteorology (e.g. simulation of a land/sea-breeze), it seems to be warranted to neglect any trend in water temperature during inundation of tidal flats.

Although the temporal variations of water temperature are weak during inundation of tidal flats, they have to be taken into account to explain the seasonal warming of water above tidal flats and the significant temperature contrast between open sea and tidal water during spring and early summer. In order to discuss these problems the heat budget of tidal water is computed from the heat exchange at the air-water interface, i.e. the residual of $Q_{rad} + Q_{lat} + Q_{sens}$, and the water-sand interface, i.e. Q_{soil}. The influence of advection of temperature on the local heat balance is estimated by subtracting the observed temperature variation during inundation from that due to local heating. For computation of heat fluxes at the air-water interface and the water-sand interface a vertically constant water temperature is assumed. Unfortunately, there were no measurements to test whether the condition of a well-mixed water mass is met. Investigations by Vugts and Zimmerman (1985), however, give some support to this assumption.

Before the local heat budget is computed, the diurnal variations of soil temperature of a tidal flat are looked at to get some idea how deep the temperature wave penetrates into a sandbar. In Figure 8 calculated vertical profiles of soil temperature of the exposed sandbar at night (1:30 LST) and daytime (13:30 LST), shortly before inundation, and of the flooded sandbar in the morning (7:30 LST) and in the evening (21:30 LST), just before recession of water, are depicted. These profiles are computed for day 6. It can be seen that heating of a sandbar during low tide penetrates down to a depth of 0.3m, approximately. The average temperature increase in this layer is $\Delta T \simeq 5K$. Therefore, about $4.8 * 10^6$ J/m^2 are absorbed by a sandbar.

Table 2: Local heat budget of tidal water. For explanation see text.

	'flood 1'	'flood 2'	'flood 3'	'flood 4'
$<Q_{rad}>$ [J/m^2]	−79	−345	−83	−249
$<Q_{lat}>$ [J/m^2]	+17	+60	+29	+12
$<Q_{sens}>$ [J/m^2]	+7	−3	+5	−2
$<Q_{soil}>$ [J/m^2]	−21	+67	−28	+55
ΔT_{A-W}[K]	+0.21	+1.06	+0.21	+0.82
ΔT_{W-S}[K]	−0.08	+0.24	−0.12	+0.19
ΔT_t[K]	−0.12	+0.70	+0.14	+0.08
ΔT_{ADV}[K]	−0.25	−0.60	+0.05	−0.93

If this energy is entirely transferred to the water during high tide, then the water temperature could increase by $\Delta T_w \simeq 0.7K$. This value can be considered as an upper bound on the warming of water due to a heated sandbar. A more careful computation follows.

Four periods of inundation of the tidal flat have been chosen for the computation of the local heat budget of tidal water: the morning ('flood 1') and the afternoon ('flood 2') high tide at day 5 as well as the morning ('flood 3') and the afternoon ('flood 4') high tide at day 6. In Table 2 the following quantities are listed: $<Q_{rad}>$, $<Q_{lat}>$, and $<Q_{sens}>$ are the energy fluxes at the air-water interface averaged over the corresponding period of inundation, $<Q_{soil}>$ is the average energy flux at the water-sand interface, ΔT_{A-W} is the temperature difference between the end and the beginning of an inundation due to energy fluxes at the air-water interface, ΔT_{W-S} is the temperature difference due to the energy flux at the water-sand interface, ΔT_t is the temperature difference recorded at the station off Pellworm, and ΔT_{ADV} is the residual of $\Delta T_{A-W} + \Delta T_{W-S}$ and ΔT_t, i.e. the influence of advection of cold or sometimes (e.g. 'flood 3') warm water on the local heat budget. From Table 2 it can be inferred that $<Q_{sens}>$ contributes least to the heat budget, whereas $<Q_{rad}>$ is the largest term. $<Q_{lat}>$ and $<Q_{soil}>$ are of comparable magni-

tude, but definitely smaller than $<Q_{rad}>$. Notice that $<Q_{soil}>$ changes sign between morning and afternoon high tide. The effect of advection varies: during 'flood 2' and 'flood 3' advection is approximately half as small as local heating, during 'flood 4' advection almost balances out local heating, and during 'flood 1' advection of cold water overcomes local heating. This is in qualitative agreement with Boxel's (1986) observation in the Dutch Wadden Sea – except for $<Q_{soil}>$. Boxel (1986) reports that $<Q_{soil}>$ is as small as $<Q_{sens}>$. However, his observation were taken at a point which was exposed to radiative heating and cooling for a much shorter time than the location off Pellworm.

It is shown that local heating of tidal water is small and is diminished and sometimes balanced out by advection. Thus, it is not surprising to observed a small, in many cases insignificant trend in water temperature during inundation. It seems, however, that during sunny weather (as at days 5 and 6) there is a temperature increase of tidal water on the average over afternoon and night or morning high tides. This would explain the seasonal warming of tidal water. The problem remains: why is tidal water warmer than the open sea?

A tentative answer to this question can be given by a satellite picture. The picture was taken by the Landsat Thematic Mapper, channel 6, on May 17th, 1986, late afternoon. The datum does not coincide with that at which the above mentioned measurements were recorded, but season and weather are similar for both dates. A temperature front is seen between water adjacent to the coast and the open sea. Here, the water near Helgoland (the island ins the lower left quarter of Figure 9) is approximately 3K colder than the water 20km east of Helgoland. The existence of such a temperature front suggests a very small exchange of water masses between open sea and tidal zone which could explain the temperature differences beween these water masses.

From the satellite picture (Figure 9), a large scale temperature contrast of 1–2K of water close to the temperature front and close to the coast is found. Obviously, the temperature difference of water within the coastal zone can be considerably smaller than the difference of open water and coastal water temperature – at least during late spring or early summer. This temperature contrast corresponds to an average temperature gradient of $\Delta T/\Delta x \sim 0.05$K/km. Assuming that the average velocity of flooding water is approximately 1m/s (Compare with Dietrich et al., 1975), then the average temperature change due to advection of cold water during a 6-hour flood at a sunny afternoon amounts to approximately $\Delta T_{ADV} \sim 1$K. This rather crude estimate is in approximate agreement with the computation for 'flood 2' and 'flood 4' in Table 2.

Figure 9 Satellite picture (contrast enhanced) from Landsat thematic mapper, channel 6, taken at May 17th, 1986, late morning. The picture was made available by Dr. Doerffer, Forschungszentrum Geesthacht.
The location of the picture is given in Figure 1.

5 Conclusion

The surface energy balance of marshy land and tidal flats has been studied by use of a simple numerical model. This model predicts the surface humidity by a simple first order differential equation. For variable weather conditions and for humid soils, the simple model is shown to agree fairly well with a more complex model. Furthermore, the predicted surface humidity comes very close to experimental data.

Meteorological data, such as wind speed, air temperature, and air humidity, which are used to drive the energy model, are taken from two masts off the German west coast on a sandbar and on a marshy island, respectively. The data were recorded during two weeks in June 1985. At this time, i.e. at the end of spring, the temperature contrast between land and sea surfaces is normally strongest. Two days with fair weather have been analysed in detail.

Concerning the surface energy fluxes, the largest differences are found in latent heat flux and in soil heat flux. While the energy flux associated with net radiation is similar for tidal flats and marshy land, the latent heat flux in the daytime above marshy land is much stronger than above tidal flats, although the air above tidal flats is always saturated. The difference of latent heat flux is attributed to a larger hydrodynamic roughness of land surfaces which causes stronger turbulent transport. The soil heat flux of land surfaces exhibits a diurnal variation, whereas the soil heat flux of sandbars is controlled by tides. During low tide the sensible heat flux is larger above sandbars than above marshy land. When inundated, sandbars give less sensible heat to the atmosphere than marshy land. Above open waters the sensible heat flux is least in comparison with tidal flats and marshy land during spring time.

Concerning surface temperature, four regimes are found. During the night, there are only slight temperature contrasts between open sea, tidal flats, and marshy land at low tide. At high tide the water temperature above tidal flats is a little bit higher than for open waters and marshy coast. By day and at high tide, there is a smooth temperature gradient between cold open waters, warmer inundated tidal flats, and still warmer marshy coast. At low tide, however, the exposed sandbars become a heat island between open waters and coast. This has not been reported by Kessler et al. (1985). They, however, consider dry land surfaces, whereas for the period being analysed in this study, the marshy land is often moistened by precipitation. Therefore, the possibility of a sandbar heat island is a new detail to be added to Kessler's et al. (1985) investigation concerning surface energy fluxes.

A further detail, which should be important in modeling the land/sea-breeze above coastal zones with extended tidal flats is the observation that water above tidal flats should generally reveal a temperature different from the open sea. From a satellite picture, a zone close to the coast is observed in which the water temperature is almost horizontally homogeneous. Futhermore, a temperature front between open sea and coastal water is seen across which a considerable temperature contrast is found. Therefore, at least for spring or early summer high tides, there is no single, steep temperature contrast between land and water, but a more or less stepped, large scale temperature gradient. Such a large scale temperature gradient could act to diffuse the land/sea-breeze.

The local heat budget to tidal water has been examined. It is shown that local heating of tidal water is small during inundation and it is diminished or sometimes balanced out by advection. Thus, the temporal variations of water temperature are weak during inundation of tidal flats. Although this small trend in water temperature has to be considered to explain the seasonal warming of tidal water, it is, on the other hand, negligibly small in comparison with temperature changes of dry surfaces such as exposed sandbars and marshy land. Hence, for many applications in mesoscale meteorology (e.g. simulation of a land/sea-breeze) it seems to be justified to neglect any trend in water temperature during inundation of tidal flats.

Presumably, the tidal heat island has a strong influence on the land/sea-breeze. One could imagine that a land/sea-breeze will be distored or will even break up into a sea/sandbar and sandbar/land-breeze. The people at the German west coast tell that thunderstorms only occur at high tide. From this study a tentative explanation for his phenomenon would be the following: For fair weather conditions, when local thunderstorms are likely to develop, the best conditions for convection are found over the dry sandbars. With rising water level, the region for optimum convection moves towards the coast and then inland along estuarian tidal flats. Numerical studies with a meoscale model are necessary to test this hypothesis.

Acknowledgements

The author wishes to thank Dr. H.-T. Mengelkamp, Forschungszentrum Geesthacht, for making the (unpublished) data available and Dr. R. Doerffer and Ms. M. Stössel, Forschungszentrum Geesthacht, for providing the satellite picture (Figure 9).

The author is also grateful to Prof. H. Grassl, Forschungszentrum Geeshacht, and Prof. H. Hinzpeter, Universität Hamburg, for discussion and Prof. H. F. Vughts, Free University Amsterdam, and another referee for valuable comments.

This study was partially supported by the 'Umweltbundesamt', Berlin.

References

Andrews, R., 1976: Wärmehaushaltsuntersuchungen im Wattgebiet der Nordseeküste. Deutsche Gewässerkundliche Mitteilungen, **20**, 117–126.

Andrews, R., 1980: Wärmeaustausch zwischen Wasser und Wattboden. Deutsche Gewässerkundliche Mitteilungen, **24**, 57–65.

Boxel, v. J., 1986: Heat balance investigation in tidal areas. PhD thesis, Free University Amsterdam, 137p.

Clarke, R. H., 1970: Recommended methods of the boundary-layer in numerical models. Austr. Met. Mag., **18**, 51–73.

Claussen, M., 1985: Die untere Randbedingung in einem numerischen Modell atmosphärischer Strömungen über unbewegten Grenzflächen. GKSS-Report, **85/E/10**, 35p; available from: Forschungszentrum Geesthacht, Max-Planck-Str., 2054 Geesthacht, F.R.G.

Claussen, M., 1986: Ein Vergleich verschiedener Modelle der Bodentemperatur und Bodenfeuchte. Ann. Met. (N.F.), **23**, 50–51.

Deardorff, J. W.; 1978: Efficient prediction of ground surface temperature and moisture with inclusion of a layer of vegetation. Jour. Geophys. Res., **83**, 1889–1903.

Diedrich, G., Kalle, K., Krauss, W., and *Siedler, G.*, 1975: Allgemeine Meereskunde. Gebrüder Bornträger, Berlin, 3rd ed., 593p.

Kasten, F. and *Czeplak, G.*; 1980: Solar and terretrial radiation dependent on the amount and type of cloud. Solar Energy, **24**, 177–189.

Kessler, R. C., Eppel, D., Pielke, R. A., and *McQueen J.*, 1985: A numerical study of the effects of a large sandbar upon sea breeze development. Arch. Met. Geoph. Biocl., **Ser. A 34**, 3–26.

Kreyszig, E., 1977: Statistische Methoden und ihre Anwendungen. Vandenhoeck und Ruprecht, Göttingen, 6th ed., 451p.

Louis, J. F., 1979: A parametric model of vertical eddy fluxes in the atmosphere. Boundary-Layer Meteorology, **17**, 187–202.

Lumley, J. L. and *Panofsky, H. A.*, 1964: The structure of atmospheric turbulence. Interscience Publ. New York, 239p.

Mast, G., Walk, O., and *Witte, N.*, 1984: Energy blance of the earth surface and resistance law at the station '30km' during PUKK. Beitr. Phys. Atmosph., **57**, 106–114.

McCumber, M. C. and *Pielke, R. A.*, 1981: Simulation of the effects of surface fluxes of heat and moisture in a mesoscale model, I. soil layer. Jour. Geophys. Res., **86**, 9929–9938.

Philip, J. R., 1975: Evaporation and moisture and heat fields in the soil. Jour. Meteorology, **14**, 354–366.

Sievers, U., Forkel, R., and *Zdunkowski, W.*, 1983: Transport equations for heat and moisture in the soil and their application to boundary-layer problems. Beitr. Phys. Atmosph. **56**, 58–83.

Vugts, H. F. and *Cannemeijer, F.*, 1981: Measurements of drag coefficients and roughness length at a sea beach. Jour. Appl. Meteor., **20**, 335–340.

Vugts, H. F. and *Zimmermann, J. T. F.*, 1985: The heat balance of a tidal flat area. Neth. J. Sea Res., **19**, 1–14.

Zilitinkevitch, S. S., 1970: Dynamics of the atmospheric boundary-layer. Hydrometeorol. Publ. House, Leningrad, 36–47.